Journal of Power Sources, 32 (1990) 389 - 396

THE LITHIUM POLYMER ELECTROLYTE BATTERY V. THE ROLES OF THE COMPOSITION AND MORPHOLOGY OF THE POSITIVE ELECTRODE

A. SELVAGGI, F. CROCE and B. SCROSATI*

Dipartimento di Chimica, Università di Roma 'La Sapienza', Rome (Italy)

(Received November 28, 1989; in revised form May 15, 1990)

Summary

The role of the composition and of the morphology of composite cathode mixtures has been analyzed in view of the development of long-life, high-efficiency, rechargeable polymer electrolyte lithium batteries.

Introduction

Intercalation compounds are presently considered as being the most promising positive electrodes for rechargeable lithium, polymer electrolyte batteries. Indeed, batteries based on the Li/TiS_2 couple are currently under study by Gauthier and co-workers [1], those based on the Li/V_6O_{13} couple by Hooper and co-workers [2], by Owens and co-workers [3], and by Lundsgaard and co-workers [4], while we [5 - 10], and other authors [11], have demonstrated the feasibility of the Li/LiV_3O_8 couple in polymer electrolyte batteries.

Effectively, there are various advantages in using these electrode materials, such as a reversible and fast electrochemical process [6], high-projected energy density values [12], and a favourable comparative cost [13].

There is a major problem associated with these cathodes when used in lithium, polymer electrolyte cells, however, *i.e.*, a progressive capacity decline upon cycling. This effect, which has been observed by various authors for polymer electrolyte batteries using different cathode materials [3, 11, 14], is not easily explained since the intercalation of lithium into insertion compounds is basically a very reversible process [12]. On the other hand, the observed decay in capacity upon cycling is a crucial aspect in the technology of polymer electrolyte batteries, and thus its solution is of primary importance. There is evidence [9] that the capacity decline may be

*Author to whom correspondence should be addressed.

0378-7753/90/$3.50

associated with a degradation of the positive electrode interface. Therefore the optimization in the composition and morphology of the cathode may be relevant to improvements in the battery cyclability. This approach is discussed in this paper with regard to LiV_3O_8-based cathodic mixtures.

Experimental

We have chosen the complex formed between poly(ethylene oxide), PEO, and lithium perchlorate, $LiClO_4$, in the preferred composition O/Li equal to 8, as typical polymer electrolyte. The electrolyte was prepared by the standard casting procedure, which included the dissolution of the components in the desired ratio in purified acetonitrile, the mixing of the solutions, and the slow evaporation of the solvent in a Teflon container. The casting and drying procedures were performed in a controlled atmosphere dry-box to avoid moisture contamination. Highly conducting (of the order of 10^{-3} - 10^{-4} S cm^{-1} at 100 °C) polymer films (of average thickness 50 - 100 μm) were obtained and stored in a dry-box. The preparation procedure of standard [15], as well as low particle-size [16] vanadium bronze, LiV_3O_8, had been described in detail by Pistoia and co-workers.

Two configurations were considered for the preparation of the composite cathode. In the first, the vanadium bronze LiV_3O_8 intercalation compound was intimately mixed with PEO and acetylene black (in the weight percent. proportion of 40:40:20) and pressed into a composite pellet. In the second configuration, small-particle-size LiV_3O_8, acetylene black, and the $(PEO)_8LiClO_4$ complex (50:15:35 wt.%) were dissolved in acetonitrile, and the composite cathode was cast to obtain a film having a plastic nature and thickness similar to those of the polymer electrolyte films.

A three-electrode cell, described in detail in a previous paper [17], was used for the investigation of the electrode kinetics. This cell was based on lithium both as the reference and as the counter electrode. A two-electrode cell of the spring-loaded, button-type was used for the cycling test. This cell was assembled by contacting a lithium disk (about 1 mm thick), one or two disks of polymer electrolyte (total thickness about 100 μm), and the positive electrode film (about 100 μm thick) between two nickel current collectors. Figure 1 illustrates this cell in section.

A similar two-electrode cell was used for the impedance measurements of the composite cathode. In this case the cell was realized by sandwiching a composite cathode film between two stainless-steel electrodes. All the cells were assembled and stored in a dry-box and kept at constant temperature (±0.5 °C) by housing them in a Buchi model TO-50 oven.

The cycling voltammetry tests were run by an in-house-built assembly which included a potentiostat, a function generator, and a personal computer. The impedance measurements were carried out using a Solartron model 1250 frequency response analyser and a Solartron model 1286 electrochemical interface. The cycling tests were performed with a galvanostat connected to an automatic voltage-controlled inverter.

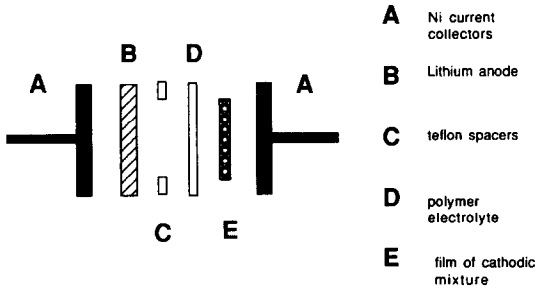

Fig. 1. Schematic design of the two electrode, polymer electrolyte, lithium cell (surface: 1.13 cm^2).

Results and discussion

The capacity decline upon cycling seems to be a typical feature of lithium, polymer electrolyte batteries using intercalation cathodes. This effect may be associated with a degradation of the cathodic material and/or with a degradation of the positive electrode interface [9]. Impedance spectroscopy is a useful tool to investigate electrode kinetics and this technique has been used here to study the polymer electrolyte/intercalation electrode interface under various conditions.

Figure 2 shows the impedance diagrams related to a freshly made (a), deeply discharged (b), and fully recharged (c) Li/LiV_3O_8 cell at 100 °C. Here, the cathode configuration was a compressed pellet of a mixture of LiV_3O_8 (the active intercalation compound), acetylene black (to enhance conductivity), and PEO, in the weight percent. proportion of 40:40:20.

It may be clearly seen that only after a complete discharge–charge cycle does the impedance diagram show a well-defined response, with a semicircle at high frequency which can be related to the Li anode–polymer electrolyte interface (with which is associated a resistance, R_a), followed by a second semicircle at intermediate frequency related to the cathode/polymer electrolyte interface (with which is associated a resistance, R_c), and a 45° Warburg line at low frequency (related to the diffusion of the intercalated lithium into the LiV_3O_8 vanadium bronze). The fact that the semicircle related to the positive interface becomes well defined only after a discharge–recharge cycle is an indication that, under the configuration used, current flow is necessary to improve the initially poor electrode/electrolyte contact conditions.

More relevant are the responses obtained upon cycling. Figure 3, which reports the impedance diagram after the 1st and the 10th deep cycles, reveals a consistent expansion of the middle frequency semicircle: this, in turn, suggesting that the positive electrode interface deteriorates in a progressive fashion. Furthermore, Fig. 4, which illustrates the impedance diagrams

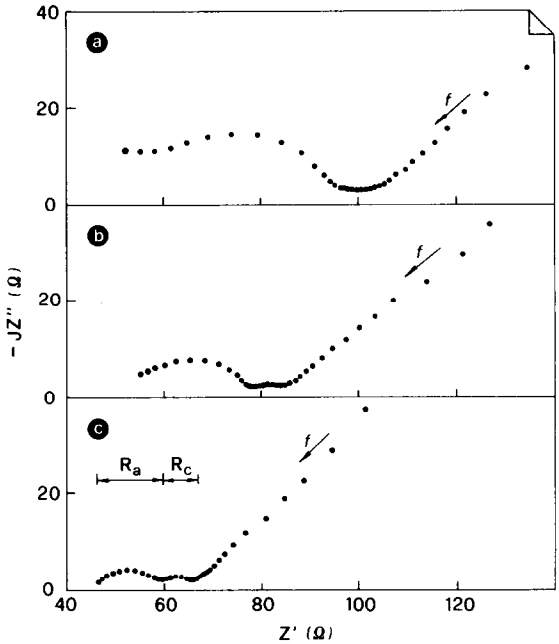

Fig. 2. Impedance response at 100 °C of an Li/LiV_3O_8 cell after being assembled (a), after a deep discharge (b), and after a complete recharge (c). Cathode configuration: compressed pellet. Charge and discharge rate: 0.1 mA cm^{-2}. Frequency range: 0.001 Hz - 65 kHz.

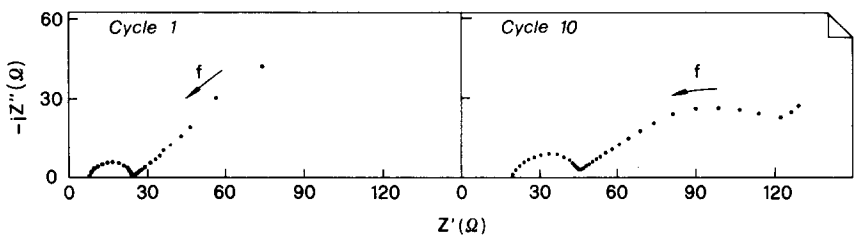

Fig. 3. Impedance response at 100 °C of an Li/LiV_3O_8 cell after the 1st (a) and the 10th (b) cycle. Cathode configuration:compressed pellet. Charge rate: 0.1 mA cm^{-2}; discharge rate: 0.2 mA cm^{-2}. Frequency range: 0.001 Hz - 65 kHz.

obtained at two progressive stages of the discharge cycle, indicates that the Warburg line tends to dominate and becomes prevalent as the discharge proceeds; this suggests that the kinetics of the intercalation process may ultimately become almost completely controlled by the diffusion of lithium in the vanadium bronze.

These results seem to show that the capacity decline of lithium, polymer electrolyte batteries may be related to a number of combined effects, including deterioration of the positive interfacial contact, structure changes at the cathodic interface and, possibly, diffusion-controlled kinetics

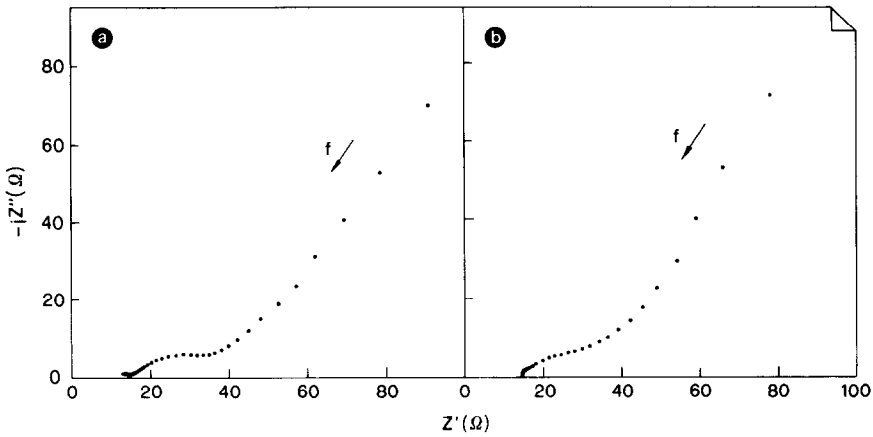

Fig. 4. Impedance response at 100 °C of a partly discharged (a), and fully discharged (b), Li/LiV_3O_8 cell. Cathode configuration: compressed pellet. Discharge rate: 0.2 mA cm^{-2}. Frequency range: 0.01 Hz - 65 kHz.

of the intercalation process. Consequently, improvements in the morphology of the cathodic mixture, with optimization of the component ratio and the particle size of the intercalation compound, should be beneficial in terms of cell behaviour.

To this end, we have considered cathodes based on small particle size LiV_3O_8 and having an overall laminated structure. To achieve this, lithium vanadium bronze with particle size reduced to less than 1 μm [16] was intimately mixed with acetylene black, PEO, and $LiClO_4$, and then cast using a procedure similar to that employed in the preparation of the polymer electrolyte. In this way, plastic-like cathodic films were obtained.

The addition of the PEO and the $LiClO_4$, besides producing a character of plasticity also provides the cathodic film with a certain amount of ionic conductivity, while acetylene black provides the electronic transport. Therefore, the film has a mixed ionic–electronic conductivity, this generally being a desirable condition for an electrode material.

Attention was initially focussed on the definition of the transport characteristics of the cathodic film. The electrical conductivity was measured by impedance spectroscopy using a cell formed from the cathodic film compressed by two stainless-steel electrodes. Figure 5, consisting of the semicircles of different amplitudes, shows the response of the cell at various temperatures. On the basis of the equivalent circuit (also reported in Fig. 5), one may associate the low-frequency intercept with the real axis to the electronic resistance, R_{EL} (mainly induced by the addition to the cathodic film of acetylene black), and the high frequency intercept to the ratio $(R_{EL} \times R_{ION})/(R_{EL} + R_{ION})$, where R_{ION} is the ionic resistance induced by the addition to the cathodic film of the PEO–$LiClO_4$ electrolyte complex. Table 1 reports the values of R_{EL} and R_{ION} obtained at various temperatures by the impedance analysis. It may be noticed that, at least in the configura-

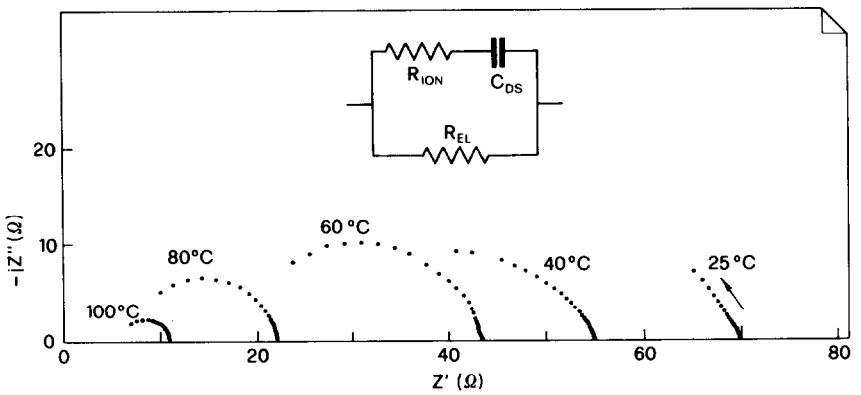

Fig. 5. Impedance plots at various temperatures of an LiV_3O_8–C–$(PEO)_8LiClO_4$ cathodic film. Stainless steel electrodes. Frequency range: 6.5 Hz - 65 kHz. The proposed equivalent circuit is shown in the inset.

TABLE 1

Ionic (R_{ION}) and electronic (R_{EL}) resistance of the LiV_3O_8, C, $(PEO)_8LiClO_4$ film at various temperatures
Film surface: 1.13 cm^2; film thickness 50 μm.

t (°C)	R_{ION} (Ω)	R_{EL} (Ω)
25	276	69
40	110	53
60	43	42
80	13	22
100	13	11
120	3	1

tion here examined, the composite cathodic film reaches homogeneity and offers acceptably low ionic and electronic resistances only at 120 °C. Therefore, batteries using this mixture should preferably operate around this temperature.

The plasticity of the cathodic film and its high ionic–electronic conductivity should, in turn, assure a good interfacial contact with the electrolyte and low *IR* drops, as well as fast electrode kinetics. The interfacial conditions have been controlled by impedance analysis. Figure 6 shows the responses of the lithium cell immediately after being assembled (a), after a deep discharge (b), and after a complete recharge (c). It may be noticed that the low frequency semicircle, which is associated with the cathodic interface, does not appreciably change upon cycling, thus confirming that the plastic configuration assures better interfacial conditions than the simple pellet (*cf.* Fig. 2).

In conclusion, the results discussed above indicate that the physical and mechanical characteristics of the cathode do indeed play a key role in the

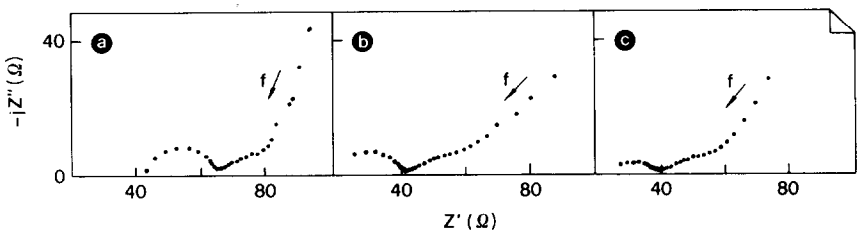

Fig. 6. Impedance response at 120 °C of an Li/LiV_3O_8 cell after being assembled (a), after deep discharge (b), and after complete recharge (c). Cathode configuration: cast film. Charge and discharge rate: 0.1 mA cm^{-2}. Frequency range: 0.001 Hz - 65 kHz.

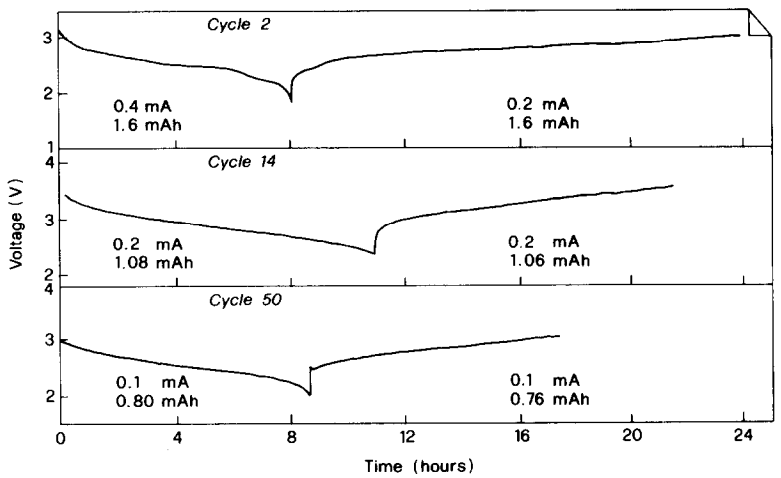

Fig. 7. Charge–discharge cycles at 120 °C of an Li/LiV_3O_8 battery under various rates. Cathodic configuration: cast film.

performance of the polymer electrolyte battery. Figure 7 illustrates the cycling profiles of a battery using the cathodic film described here. Well-defined charge and discharge profiles, with good coulombic efficiencies, are obtained for several cycles, this finally proving the consistent enhancement in cell behaviour resulting from the use of the improved cathode configuration. This conclusion is further supported by considering that cycling tests performed in our laboratory on similar batteries made with compressed pellets, under similar conditions of charge and discharge rate and voltage limits, gave much poorer cycling response. This is clearly shown by Fig. 8 which compares the initial cycling behaviour of cells using the two types of cathode morphology.

Acknowledgements

This work has been carried out with the financial support of the Consiglio Nazionale delle Richerche (CNR), Progetto Finalizzato Energetica 2

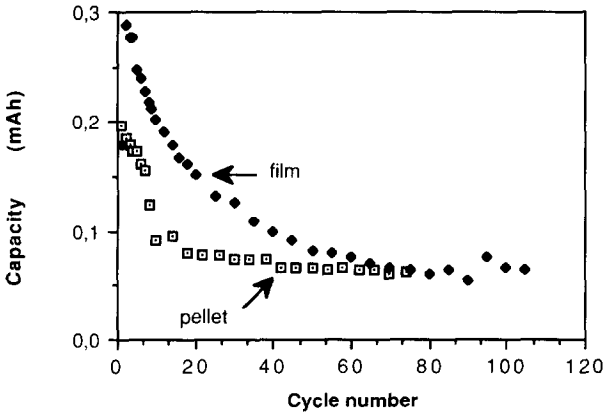

Fig. 8. Initial cycling behaviour at 120 °C of Li/LiV_3O_8 batteries using cast film and compressed pellet as the cathode configuration. Charge rate: $C/10$; discharge rate: $C/5$.

(PFE2), contract CNR No 88.01359.59 and of the Commission of the European Communities, Contract EN3E-0145-I.

References

1 M. Gauthier, *3rd Int. Seminar Lithium Batteries, Florida, U.S.A., March, 1987.*
2 A. Hooper and B. C. Tofield, *J. Power Sources, 11* (1984) 33.
3 M. Z. A. Munshi and B. B. Owens, *Solid State Ionics, 20* (1988) 41.
4 J. S. Lundsgaard, S. Yde-Andersen, R. Koksbang, D. R. Shackle, R. A. Austin and D. Fauteux, *Proc. 2nd Int. Symp. Polymer Electrolytes (ISPE 2), Siena, Italy, June, 1989*, Elsevier, London, 1990, p. 395.
5 F. Bonino, M. Ottaviani, B. Scrosati and G. Pistoia, *J. Electrochem. Soc., 135* (1988) 12.
6 B. Scrosati, *Br. Polym. J., 20* (1988) 219.
7 F. Bonino, A. Selvaggi and B. Scrosati, *Solid State Ionics, 28 - 30* (1988) 853.
8 B. Scrosati, A. Selvaggi, F. Croce and Wang Gang, *J. Power Sources, 24* (1988) 287.
9 B. Scrosati, *J. Electrochem. Soc., 136* (1989) 2774.
10 B. Scrosati, A. Selvaggi and B. B. Owens, *Prog. Batteries Solar Cells*, in press.
11 K. West, B. Zachau-Christiansen and T. Jacobsen, *J. Power Sources, 14* (1987) 165.
12 B. Scrosati, in J. R. MacCallum and C. A. Vincent (eds.), *Polymer Electrolyte Review I*, Elsevier Applied Science, London, 1987, pp. 315 - 346.
13 B. B. Owens, *EPRI Rep. AP-5218*, June, 1987.
14 L. Yang, R. Zhou and Q. Liu, in B. V. R. Chowdari and S. Radhakrishan (eds.), *Solid State Ionic Devices*, World Scientific Publ., Singapore, 1988, p. 469.
15 G. Pistoia, S. Panero, M. Tocci, R. V. Moshtev and V. Manev, *Solid State Ionics, 13* (1984) 311.
16 G. Pistoia, M. Pasquali, Y. Geronov, V. Manev and R. V. Moshtev, *J. Power Sources, 27* (1989) 35.
17 F. Bonino, B. Scrosati, A. Selvaggi, J. Evans and C. A. Vincent, *J. Power Sources, 18* (1985) 75.